



## RESEARCH LETTER

10.1002/2016GL070153

## Key Points:

- Organics contribute to 30–40% of stratospheric aerosol burden
- The increase in stratospheric aerosol optical depth (AOD) is ~12% of the total atmospheric AOD change since 1850
- Radiative forcing from stratospheric aerosol is ~21% of the total direct aerosol radiative forcing since 1850

## Supporting Information:

- Supporting Information S1
- Figure S1
- Figure S2
- Figure S3

## Correspondence to:

P. Yu,  
pengfei.yu@noaa.gov

## Citation:

Yu, P., D. M. Murphy, R. W. Portmann, O. B. Toon, K. D. Froyd, A. W. Rollins, R.-S. Gao, and K. H. Rosenlof (2016), Radiative forcing from anthropogenic sulfur and organic emissions reaching the stratosphere, *Geophys. Res. Lett.*, *43*, 9361–9367, doi:10.1002/2016GL070153.

Received 22 JUN 2016

Accepted 29 AUG 2016

Accepted article online 31 AUG 2016

Published online 14 SEP 2016

## Radiative forcing from anthropogenic sulfur and organic emissions reaching the stratosphere

Pengfei Yu<sup>1,2</sup>, Daniel M. Murphy<sup>1</sup>, Robert W. Portmann<sup>1</sup>, Owen B. Toon<sup>3,4</sup>, Karl D. Froyd<sup>1,2</sup>, Andrew W. Rollins<sup>1,2</sup>, Ru-Shan Gao<sup>1</sup>, and Karen H. Rosenlof<sup>1</sup>

<sup>1</sup>Earth System Research Laboratory, National Oceanic and Atmospheric Administration, Boulder, Colorado, USA,

<sup>2</sup>Cooperative Institute for Research in Environmental Sciences, University of Colorado Boulder, Boulder, Colorado, USA,

<sup>3</sup>Department of Atmospheric and Oceanic Sciences, University of Colorado Boulder, Boulder, Colorado, USA, <sup>4</sup>Laboratory for Atmospheric and Space Physics, University of Colorado Boulder, Boulder, Colorado, USA

**Abstract** Stratospheric aerosols cool the Earth by scattering sunlight. Although sulfuric acid dominates the stratospheric aerosol, this study finds that organic material in the lowermost stratosphere contributes 30–40% of the nonvolcanic stratospheric aerosol optical depth (sAOD). Simulations indicate that nonvolcanic sAOD has increased 77% since 1850. Stratospheric aerosol accounts for 21% of the total direct aerosol radiative forcing (which is negative) and 12% of the total aerosol optical depth (AOD) increase from organics and sulfate. There is a larger stratospheric influence on radiative forcing (i.e., 21%) relative to AOD (i.e., 12%) because an increase of tropospheric black carbon warms the planet while stratospheric aerosols (including black carbon) cool the planet. Radiative forcing from nonvolcanic stratospheric aerosol mass of anthropogenic origin, including organics, has not been widely considered as a significant influence on the climate system.

### 1. Introduction

Aerosols cool the Earth by scattering sunlight. In the troposphere, sulfate and organic compounds are key aerosol components [Murphy *et al.*, 2006; Zhang *et al.*, 2007]. In the stratosphere, sulfuric acid has long been thought to be the primary aerosol constituent [Junge and Manson, 1961; Myhre *et al.*, 2004; English *et al.*, 2011; Neely *et al.*, 2013]. Most prior studies of stratospheric aerosol have focused on sulfate from exceptional volcanic events [English *et al.*, 2013], moderate volcanic eruptions [Neely *et al.*, 2013; Andersson *et al.*, 2015; Mills *et al.*, 2014], or tropospheric emissions [Myhre *et al.*, 2004; Solomon *et al.*, 2011]. However, airborne observations [Murphy *et al.*, 2014; Froyd *et al.*, 2009] show that organic compounds make up 5–50% of lower stratospheric aerosol mass. Additionally, substantial contributions from organic aerosols (OA) have been observed and modeled in the summertime Asian upper troposphere and lower stratosphere (UTLS) [Vernier *et al.*, 2015; Yu *et al.*, 2015b]. Particles in the stratosphere below ~15 km altitude contribute 20 to 80% of the nonvolcanic total stratospheric optical depth in the extra tropics [Ridley *et al.*, 2014]. Organic material in the lowermost stratosphere is not distinguishable from sulfate by satellite instruments and has been largely ignored by the stratospheric modeling community. The stratospheric concentrations of both sulfates and organics likely have changed in time in response to changes in surface conditions and emissions, thereby moderating surface temperature increases due to greenhouse gas increases.

### 2. Methods

This study uses a sectional aerosol microphysics model, Community Aerosol and Radiation Model for Atmospheres (CARMA), coupled with the National Science Foundation/Department of Energy/National Center for Atmospheric Research Community Earth System Model (CESM) to investigate stratospheric aerosols [Yu *et al.*, 2015a; Toon *et al.*, 1988]. We first demonstrate that our simulations agree with available observational data within the measurement uncertainties. Then, using runs for present and preindustrial conditions, we quantify the aerosol composition, budget, and optical properties in the stratosphere.

Properties of stratospheric aerosols are analyzed using the general circulation model CESM version 1 (CESM1) coupled with CARMA [Yu *et al.*, 2015a; Toon *et al.*, 1988]. CESM/CARMA includes primary emitted organics, secondary organics, dust, sea salt, black carbon, and sulfate [Yu *et al.*, 2015a]. CARMA includes two groups of aerosols. The first group consists of pure sulfate with 20 size bins having radii ranging from 0.2 nm to

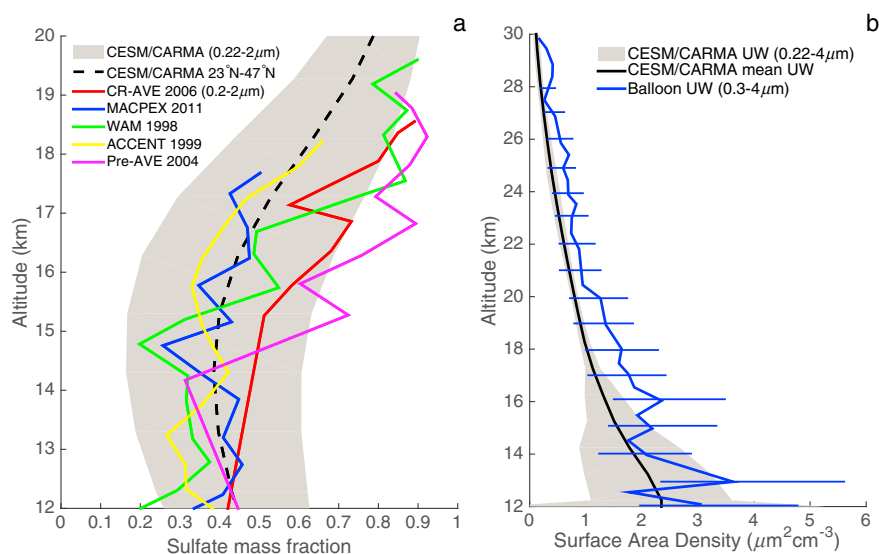


**Figure 1.** (a) The ratio of sulfate mass to total mass (sulfate plus OA; from 0.2  $\mu\text{m}$  to 2  $\mu\text{m}$  in particle diameter) from five different field campaigns from 1998 to 2011 (see section 2 for details of the campaigns). CESM/CARMA simulations (dashed black line; from 0.22  $\mu\text{m}$  to 2.0  $\mu\text{m}$  in particle diameter) are plotted as temporal averages from 2000 to 2010. Both observations and simulations are between 23°N and 47°N. Shading denotes temporal and latitudinal variability (1 standard deviation) in the model; (b) balloon-borne particle surface area density ( $\mu\text{m}^2 \text{cm}^{-3}$ ) measurements at 41°N, 105°W (Laramie, Wyoming; from 0.3  $\mu\text{m}$  to 4  $\mu\text{m}$ ) are shown by the blue line for the low volcanic impact period of 1997 to 2005 with 1 standard deviation denoted by horizontal lines [Kovilakam and Deshler, 2015]. The black line shows the mean of CESM/CARMA simulations (from 0.22  $\mu\text{m}$  to 4  $\mu\text{m}$ ) for the model grid box containing the observed point. Shading denotes 1 standard deviation of simulations averaged from 2000–2005.

1.3  $\mu\text{m}$ . These are particles formed through nucleation and condensation of water and sulfuric acid vapor. The second group consists of mixed aerosols with 20 size bins having radii ranging from 50 nm to 8.7  $\mu\text{m}$ . These are particles containing mixtures of organics, black carbon, sea salt, dust, and condensed sulfate. Separate size bins for pure sulfate and mixed organic-sulfate particles are consistent with single particle data in the lower stratosphere [Murphy *et al.*, 2014]. The optical properties of the aerosols in CESM/CARM are estimated using Mie scattering code based on inputs of particle size, relative humidity, and composition [Yu *et al.*, 2015a].

We simulated secondary organic aerosol (SOA) gas-particle partitioning using a volatility basis set method (four volatility bins) [Pye *et al.*, 2010]. Five volatile organic compounds (VOCs) including isoprene, monoterpene, benzene, xylene, and toluene are tracked in CESM as SOA precursors [Emmons *et al.*, 2010].

We run CESM/CARMA with a horizontal resolution of  $1.9^\circ \times 2.5^\circ$  and 56 levels vertically (26 vertical levels are above 200 hPa). Simulations for the time period 2000 to 2013 and 1850 to 1854 were conducted; only results after a 3 year model spin up period are considered. Emissions of  $\text{SO}_2$ , VOCs, and primary organic aerosol (POA) used in the simulations are from the Climate Model Intercomparison Project #5 (CMIP5) [Lamarque *et al.*, 2010]. Greenhouse gases for 1850–1854 and 2000–2013 are from the Intergovernmental Panel on Climate Change Fifth Assessment Report [Boucher *et al.*, 2013]. Carbonyl sulfide (OCS) is specified with a constant surface concentration of 510 pptv for present day [Chin and Davis, 1995] and 373 pptv for 1850 [Aydin *et al.*, 2002]. Volcanic emissions are not included in this study; here we exclusively test nonvolcanic contributions to aerosols in the stratosphere.

Figure 1a shows data from the aircraft born Particle Analysis by Laser Mass Spectrometry (PALMS) collected during the following missions: WB57 Aerosol Mission (WAM, April–May 1998), Atmospheric Chemistry of Combustion Emissions Near the Tropopause (ACCENT, September–October 1999), Pre-Aura Validation Experiment (Pre-AVE, January–February 2004), Costa Rica Aura Validation Experiment (CR-AVE, January–February 2006), and the Mid-latitude Airborne Cirrus Properties Experiment (MACPEX, March–April 2011). PALMS ion ratios of sulfate and organic peaks have been converted to mass fractions using both comparisons

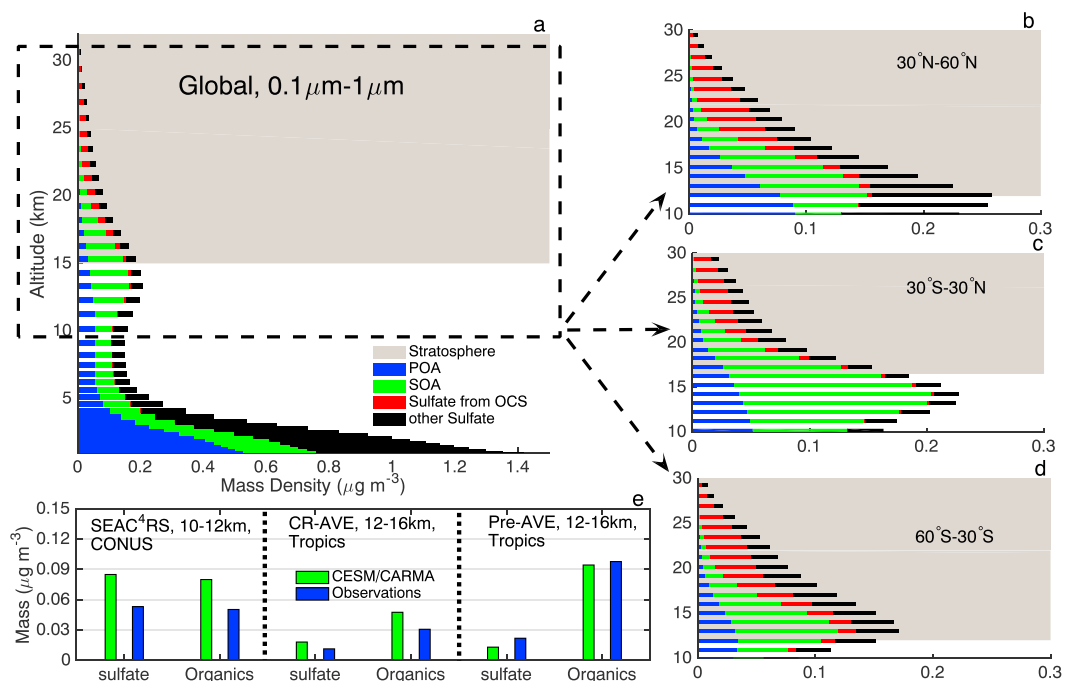


**Figure 2.** (a) Simulated global average nonvolcanic aerosol composition for 2000–2010 for aerosol diameter ranging from 0.1  $\mu\text{m}$  to 1  $\mu\text{m}$ . Deep blue bars denote POA mass concentrations (unit:  $\mu\text{g m}^{-3}$ ), green bars denote SOA, red bars denote sulfate from OCS, and black bars denote sulfate from other sources including surface emitted  $\text{SO}_2$  and DMS. (b–d) Same as Figure 2a but averaged for Northern Hemisphere midlatitudes (30°N–60°N), tropics (30°S–30°N), and Southern Hemisphere midlatitudes (60°S–30°S). (e) Mass density of sulfate and organics in the upper troposphere modeled (green bars) and measured (blue bars) from three different field campaigns including Studies of Emissions, Atmospheric Composition, Clouds and Climate Coupling by Regional Surveys (SEAC<sup>4</sup>RS) [Toon *et al.*, 2016], CR-AVE, and Pre-AVE. Note both CR-AVE and Pre-AVE campaigns were based from Costa Rica but measured quite different air masses [Froyd *et al.*, 2009].

to other measurements [Murphy *et al.*, 2006] and laboratory calibrations of mixed particles with various amounts of sulfate, organic acids, and humic-like substances, a surrogate for highly oxidized organic aerosol compounds (Figure S3 in the supporting information). Nitrate and ammonium are not considered in the mass fraction estimates.

PALMS organic and sulfate mass fractions were combined with coincident measurements of aerosol size and concentration [Froyd *et al.*, 2009; Wilson *et al.*, 2008; Ziemba *et al.*, 2013] to give absolute mass concentrations of organic and sulfate aerosol. Dust, sea salt, and soot particles were excluded. We run the model offline with observed winds and temperatures to compare with observations

### 3. Results

In Figure 1b, we compare simulated particle surface area density (SAD) with observations from the University of Wyoming balloon-borne optical particle counter [Kovilakam and Deshler, 2015]. Above 12 km our simulated SAD is biased  $\sim 25\%$  low with respect to the mean Wyoming profile but falls within one sample standard deviation for each altitude bin. Measurements from the PALMS instrument are compared with the modeled aerosol composition in the UTLS region in Figure 1a. Observations are from five field campaigns from 1998 to 2011 covering latitudes from 23°N to 47°N. Figure 1a shows that simulations (from 0.22  $\mu\text{m}$  to 2  $\mu\text{m}$  in particle diameter) are within the measured range (from 0.2  $\mu\text{m}$  to 2  $\mu\text{m}$  in particle diameter) of sulfate mass fraction below 20 km in altitude where observations show the majority of organic mass is located. The sulfate mass accounts for 30–50% of nonrefractory particles in the UTLS below 15 km, above which sulfate starts to dominate. In addition to in situ measurements, modeled stratospheric AOD agrees with long-term measurements by lidar and satellites (see Figures S1 and S2 in the supporting information).

In Figure 2a, we show global averages of the modeled primary organic aerosol (POA, including anthropogenic and biomass burning organic aerosols), secondary organic aerosol (SOA, including organic aerosols

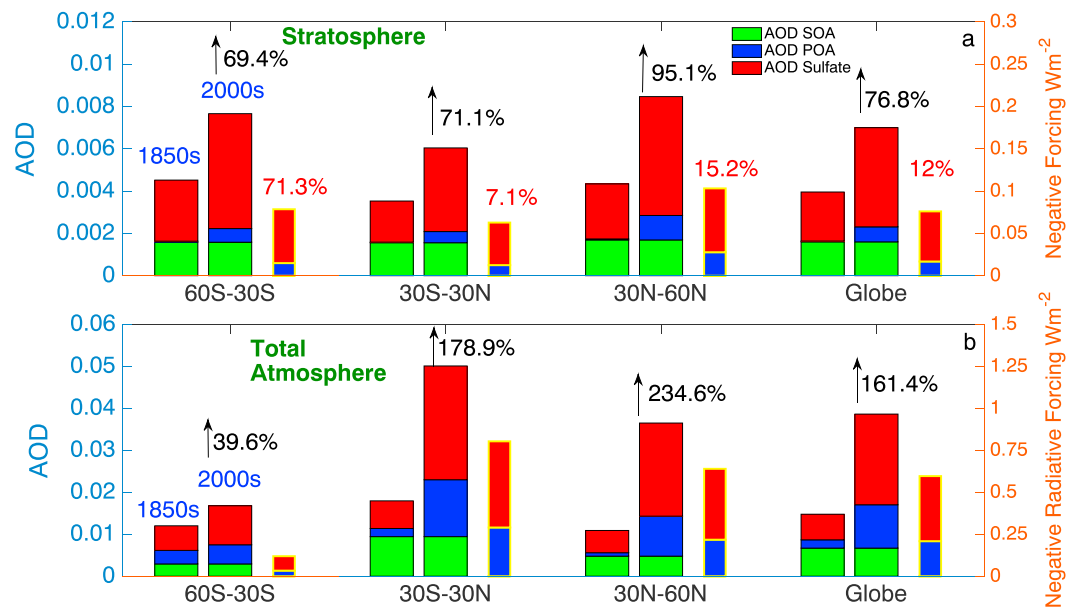


**Figure 3.** (a) Simulated stratospheric AOD of POA (blue bars), SOA (green bars), and sulfate (red bars) averaged for different latitude bands (60°S–30°S, 30°S–30°N, 30°N–60°N, and the globe). For each latitude band, the left stacked bars denote model output from the 1850s run, the middle stacked bars denote model output from the 2000s run, and the rightmost stacked bars denote the difference between 2000s and 1850s. Percent of stratospheric AOD change since 1850s (with respect to sAOD in 1850s) are denoted in black numbers above the middle stacked bars. The red numbers the percent of total optical depth due to stratospheric aerosols. (b) Same as Figure 3a but for the total depth of the atmosphere.

generated from oxidation of anthropogenic and biogenic volatile organic compounds, VOCs) and sulfate (from OCS, surface emitted  $\text{SO}_2$ , and dimethyl sulfide (DMS)). Oxidation of DMS is described in *Lamarque et al.* [2012] and *Yu et al.* [2015a]. The simulated total OA (the sum of SOA and POA) is slightly larger than the sulfate mass density in the UTLS up to 18 km; sulfate dominates above 19 km. Figure 2a shows that OA is at least half of the total aerosol mass in the UTLS (12–17 km) for the global average. In general, surface emitted  $\text{SO}_2$  is the main source of sulfate aerosol below 20 km, while above 20 km OCS oxidation dominates. In the model, formation of sulfate aerosol through tropospheric  $\text{SO}_2$  occurs primarily below the tropopause and is transported to the lower stratosphere as sulfate. Our calculations (Figure 2a) suggest that OCS is responsible for ~50% of the nonvolcanic sulfate in the stratosphere.

To show latitudinal variability, aerosol composition averaged for several latitude bands is plotted in Figures 2b–2d. Near the tropopause, the highest POA and sulfate mass concentrations are found in Northern Hemisphere midlatitudes resulting from anthropogenic emissions. The highest SOA mass is found in the tropics resulting from biogenic emission of VOCs from forests (i.e., the Amazon and Southeast Asia). Figure 2e shows that modeled UTLS composition is comparable with the limited in situ measurements available in both the tropics and midlatitudes.

In order to examine natural and anthropogenic sources of stratospheric nonvolcanic aerosol, a preindustrial case was run using the emissions from the Climate Model Intercomparison Project #5 (CMIP5) [*Lamarque et al.*, 2010]. The model was run for 5 years using emissions of greenhouse gases, carbonaceous aerosols,  $\text{SO}_2$ , and VOCs representing the 1850s. Global mean natural emissions of  $\text{SO}_2$ , POA, and VOCs varied little between 1850 and 2000, while anthropogenic emissions increased significantly for POA (by 80%) and  $\text{SO}_2$  (by a factor of 65).

The stratospheric aerosol optical depth (sAOD) for the two time periods, subdivided by the mass fraction of each type of aerosol, is shown in Figure 3a, while total column AOD is shown in Figure 3b. Significant changes in of sAOD (about 70% to 95% increases with respect to the sAOD in 1850s) are shown for all latitude bands; the global mean increase is 77%. The change in the stratospheric sulfate aerosol burden since 1850 suggests that anthropogenic sources produce ~50% of present-day stratospheric nonvolcanic sulfate. The remaining

nonvolcanic stratospheric sulfate comes from natural sources of OCS, DMS and tropospheric biomass burning. While changing tropospheric  $\text{SO}_2$  emissions are responsible for  $\sim 75\%$  of the AOD increase in the stratosphere, the POA contribution is also significant. Modeled changes of SOA in the stratosphere are negligible due to the limited change of global emissions of biogenic VOCs since 1850 [Acosta Navarro *et al.*, 2014]. The ratio of stratospheric aerosol optical depth increase (Figure 3a) relative to the total AOD column increase (Figure 3b) from both  $\text{SO}_2$  and POA emissions since 1850 is greatest at midlatitudes of the Southern Hemisphere (71.3%), while it is modest in midlatitudes of the Northern Hemisphere (15.2%) and in the tropics (7.1%). The large midlatitude stratospheric aerosol increase is a consequence of two factors. First, anthropogenic pollution that reaches the stratosphere is transported efficiently toward both poles whereas pollution that remains solely in the troposphere is not efficiently transported poleward. Second, the tropopause is lower at high latitudes, so the high-latitude stratosphere has significantly more mass and thus higher aerosol optical depth as compared to lower latitudes. Our study suggests that increases in stratospheric AOD are a significant component of the total column AOD increase (troposphere plus stratosphere) since the preindustrial period, making up 12% of the global AOD change. Likewise, 16% of the sulfate mass change, and 10% of the POA mass change induced by both sulfur and primary organic emissions since 1850, lies in the stratosphere.

The contribution of sAOD to climate change can be calculated through radiative forcing calculations. We estimate stratospheric radiative forcing by multiplying the stratospheric component of AOD by a conversion factor of  $25 \text{ W m}^{-2}$  per unit AOD [Hansen *et al.*, 2005; Solomon *et al.*, 2011], with a range from 20 to 30 [Hansen *et al.*, 2005; Larson and Portmann, 2016]. Note that the conversion factor varies with particle size distribution (more fine mode particles in present-day than 1850s) and surface albedo [Murphy, 2013]. Our simulations suggest that present-day nonvolcanic stratospheric aerosol produces a global forcing of  $-0.175 \text{ W m}^{-2}$  (more negative by  $-0.072 \text{ W m}^{-2}$  since 1850). OA is responsible for 30–40% of the current stratospheric aerosol forcing.

Our estimate of the stratospheric radiative forcing since 1850 is about 50% higher than the forcing by anthropogenic stratospheric sulfate estimated by Myhre *et al.*, [2004], partly because that study did not include stratospheric organics. Changes in stratospheric aerosol are implicitly included in some CMIP5 models but not others. The CMIP5 models [Boucher *et al.*, 2013; Charlton-Perez *et al.*, 2013] include a variety of vertical resolutions (model top ranges from  $5.1 \times 10^{-6}$  hPa to 10 hPa with the number of vertical levels above 200 hPa ranging from 3 to 63). The low vertical resolution models may not be sufficient to adequately resolve stratosphere processes [Charlton-Perez *et al.*, 2013]. Thus, the stratospheric aerosol budget and its radiative forcing may not be well simulated.

The aerosol radiative forcing since 1850 of  $-0.072 \text{ W m}^{-2}$  due to organics and sulfate in the stratosphere is 21% of the estimated negative radiative forcing for direct aerosol-radiation interaction of  $-0.35 \text{ W m}^{-2}$  [Boucher *et al.*, 2013] concerning the entire aerosol system. Here we use the Intergovernmental Panel on Climate Change (IPCC) estimate for the combined direct aerosol radiative forcing since our model calculations do not include changes in nitrate and dust. The aerosol direct forcing induced by the change of organic aerosol and sulfate in the entire atmospheric column in our model is  $-0.62 \text{ W m}^{-2}$  (Figure 3b), which is comparable to that estimated by Boucher *et al.*, [2013] of  $-0.52$  (from  $-1.23$  to  $0.17$ )  $\text{W m}^{-2}$ . Details of the forcing calculated and quoted in this study are listed in Table S1 in the supporting information.

#### 4. Discussion

Why is the stratospheric contribution to radiative forcing (21%) so much larger than the contribution to optical depth (12%)? The main reason is that warming from black carbon balances the majority of the direct radiative forcing from sulfate and organic aerosol in the troposphere [Boucher *et al.*, 2013]. It should be emphasized that this cancellation applies only to the troposphere; black carbon in the stratosphere cools the Earth [Ban-Weiss *et al.*, 2012; Samset and Myhre, 2015; Mills *et al.*, 2014]. Therefore, the *net* forcing by anthropogenic aerosols in the stratosphere is especially important.

The uncertainty in a radiative forcing calculation comes from uncertainty about both recent and past atmospheres. Only present-day stratospheric aerosol size distribution and composition model results can be compared with observations. We find that with the present-day simulations, the model may

underestimate sulfate area density by 25% and overestimate stratospheric AOD by 50%. Large uncertainties remain regarding the formation and aging of SOA, brown carbon, and other aerosol. In addition, another important uncertainty is the estimation of emissions, especially organics in the 1850s [Lamarque et al., 2010]. There are also uncertainties in possible changes in vertical transport and microphysical processes (e.g., wet deposition); as well as optical properties, especially for organics, which in the model are assumed to be nonabsorbing. Because of the high uncertainties on vertical transport and wet scavenging of black carbon in global models [Schwarz et al., 2013], our estimated stratospheric aerosol forcing does not include the cooling effect of stratospheric black carbon (up to  $-0.05 \text{ W m}^{-2}$ , see supporting information for estimation methods).

## 5. Summary

A sectional aerosol model (CARMA) coupled with CESM is used to study the nonvolcanic stratospheric aerosol compositions and their radiative forcing. The model compares well with the limited available observations of aerosol composition in the stratosphere. We find that in addition to sulfate, there are 30–40% of organic aerosols in the stratosphere, primarily in the lowermost stratosphere. Simulations suggest that stratospheric AOD has increased by 77% since 1850, which is about 12% of the AOD change in the total atmosphere. We estimate an aerosol radiative forcing of  $-0.072 \text{ W m}^{-2}$  in the stratosphere since 1850, which is about 21% of the aerosol direct radiative forcing of the full depth of the atmosphere estimated by Intergovernmental Panel on Climate Change (IPCC) [Boucher et al., 2013]. The relative higher contribution of stratospheric aerosols to radiative forcing (21%) than to AOD change (12%) since 1850 is because black carbon (BC) in the troposphere warms the Earth; while BC in the stratosphere cools the Earth [Ban-Weiss et al., 2012; Samset and Myhre, 2015; Mills et al., 2014]. A small amount of BC in the stratosphere could significantly increase the radiative forcing estimate, but observations are presently lacking to support this. Our results highlight the importance of organic compounds in addition to sulfate to the stratospheric aerosol budget and to anthropogenic climate change.

## Acknowledgments

The CESM project is supported by the National Science Foundation and the Office of Science (BER) of the U.S. Department of Energy. NOAA and CIRES authors of this study were supported by NOAA's Climate Program Office. O.B.T. was supported by NASA grant NNX14AR56G. We thank John E. Barnes for discussions on the NOAA/Mauna Loa Observatory lidar observations, which are available at <http://www.esrl.noaa.gov/gmd/obop/mlo/livedata/livedata.html>, and Louisa Emmons for providing emissions data sets of chemicals from 2000 to 2013. We thank James C. Wilson providing aerosol data on AVE field campaigns. We thank Luke Ziemba and Bruce Anderson for aerosol size distribution data from SEAC<sup>4</sup>RS. The University of Wyoming data are available at [http://www-das.uwyo.edu/~deshler/Data/Aer\\_Meas\\_Wy\\_read\\_me.htm](http://www-das.uwyo.edu/~deshler/Data/Aer_Meas_Wy_read_me.htm). PALMS data are publicly available from <http://espoarchive.nasa.gov/>. We appreciate comments from anonymous reviews that improved the paper and thank David W. Fahey for helpful discussions.

## References

- Acosta Navarro, J. C., S. Smolander, H. Struthers, E. Zorita, A. M. L. Ekman, J. O. Kaplan, A. Guenther, A. Arneth, and I. Riipinen (2014), Global emissions of terpenoid VOCs from terrestrial vegetation in the last millennium, *J. Geophys. Res. Atmos.*, *119*, 6867–6885, doi:10.1002/2013JD021238.
- Andersson, S. M., et al. (2015), Significant radiative impact of volcanic aerosol in the lowermost stratosphere, *Nat. Commun.*, *6*, doi:10.1038/ncomms8692.
- Aydin, M., et al. (2002), Preindustrial atmospheric carbonyl sulfide (OCS) from an Antarctic ice core, *Geophys. Res. Lett.*, *29*(9), doi:10.1029/2002GL014796.
- Ban-Weiss, G. A., L. Cao, G. Bala, and K. Caldeira (2012), Dependence of climate forcing and response on the altitude of black carbon aerosols, *Clim. Dyn.*, *38*, 897–911, doi:10.1007/s00382-011-1052-y.
- Boucher, O., et al. (2013), In *Climate Change 2013: The Physical Science Basis. Contribution of Working Group I to the Fifth Assessment Report of the Intergovernmental Panel on Climate Change*, edited by T. F. Stocker et al., pp. 574, Cambridge Univ. Press, Cambridge.
- Charlton-Perez, A. J., et al. (2013), On the lack of stratospheric dynamical variability in low-top versions of the CMIP5 models, *J. Geophys. Res. Atmos.*, *118*, 2494–2505, doi:10.1002/jgrd.50125.
- Chin, M., and D. D. Davis (1995), A reanalysis of carbonyl sulfide as a source of stratospheric background sulfur aerosol, *J. Geophys. Res.*, *100*(D5), 8993–9005, doi:10.1029/95JD00275.
- Emmons, L. K., et al. (2010), Description and evaluation of the Model for Ozone and Related chemical Tracers, version 4 (MOZART-4), *Geosci. Model Dev.*, *3*, 43–67, doi:10.5194/gmd-3-43-2010.
- English, J. M., O. B. Toon, M. J. Mills, and F. Yu (2011), Microphysical simulations of new particle formation in the upper troposphere and lower stratosphere, *Atmos. Chem. Phys.*, *11*(17), 9303–9322, doi:10.5194/acp-11-9303-2011.
- English, J. M., O. B. Toon, and M. J. Mills (2013), Microphysical simulations of large volcanic eruptions: Pinatubo and Toba, *J. Geophys. Res. Atmos.*, *118*, 1880–1895, doi:10.1002/jgrd.50196.
- Froyd, K. D., D. M. Murphy, T. J. Sanford, D. S. Thomson, J. C. Wilson, L. Pfister, and L. Lait (2009), Aerosol composition of the tropical upper troposphere, *Atmos. Chem. Phys.*, *9*(13), 4363–4385.
- Hansen, J., et al. (2005), Efficacy of climate forcings, *J. Geophys. Res.*, *110*, D18104, doi:10.1029/2005JD005776.
- Junge, C. E., and J. E. Manson (1961), Stratospheric aerosol studies, *J. Geophys. Res.*, *66*(7), 2163–2182, doi:10.1029/JZ066i007p02163.
- Kovilakam, M., and T. Deshler (2015), On the accuracy of stratospheric aerosol extinction derived from in situ size distribution measurements and surface area density derived from remote SAGE II and HALOE extinction measurements, *J. Geophys. Res. Atmos.*, *120*, 8426–8447, doi:10.1002/2015JD023303.
- Lamarque, J.-F., et al. (2010), Historical (1850–2000) gridded anthropogenic and biomass burning emissions of reactive gases and aerosols: Methodology and application, *Atmos. Chem. Phys.*, *10*, 7017–7039, doi:10.5194/acp-10-7017-2010.
- Lamarque, J.-F., et al. (2012), CAM-chem: Description and evaluation of interactive atmospheric chemistry in the Community Earth System Model, *Geosci. Model Dev.*, *5*, 369–411, doi:10.5194/gmd-5-369-2012.
- Larson, E. J. L., and R. W. Portmann (2016), A temporal kernel method to compute effective radiative forcing in CMIP5 transient simulations, *J. Clim.*, *29*, 1497–1509, doi:10.1175/JCLI-D-15-0577.1.

- Mills, M. J., O. B. Toon, J. Lee-Taylor, and A. Robock (2014), Multidecadal global cooling and unprecedented ozone loss following a regional nuclear conflict, *Earth's Future*, 2, doi:10.1002/2013EF000205.
- Mills, M. J., et al. (2016), Global volcanic aerosol properties derived from emissions, 1990–2014, using CESM1(WACCM), *J. Geophys. Res. Atmos.*, 121, 2332–2348, doi:10.1002/2015JD024290.
- Murphy, D. M., et al. (2006), Single-particle mass spectrometry of tropospheric aerosol particles, *J. Geophys. Res.*, 111, doi:10.1029/2006JD007340.
- Murphy, D. M., K. D. Froyd, J. P. Schwarz, and J. C. Wilson (2014), Observations of the chemical composition of stratospheric aerosol particles, *Q. J. R. Meteorol. Soc.*, 140, 1269–1278, doi:10.1002/qj.2213.
- Murphy, D. M. (2013), Little net clear-sky radiative forcing from recent regional redistribution of aerosols, *Nat. Geosci.*, 6, 258–262, doi:10.1038/ngeo1740.
- Myhre, G., et al. (2004), The radiative effect of the anthropogenic influence on the stratospheric sulfate aerosol layer, *Tellus B*, 56(3), doi:10.1111/j.1600-0889.2004.00106.x.
- Neely, R. R., III, et al. (2013), Recent anthropogenic increases in SO<sub>2</sub> from Asia have minimal impact on stratospheric aerosol, *Geophys. Res. Lett.*, 40, doi:10.1002/grl.50263.
- Pye, H. O. T., A. W. H. Chan, M. P. Barkley, and J. H. Seinfeld (2010), Global modeling of organic aerosol: The importance of reactive nitrogen (NO<sub>x</sub> and NO<sub>3</sub>), *Atmos. Chem. Phys.*, 10, 11,261–11,276, doi:10.5194/acp-10-11261-2010.
- Ridley, D. A., et al. (2014), Total volcanic stratospheric aerosol optical depths and implications for global climate change, *Geophys. Res. Lett.*, 41, 7763–7769, doi:10.1002/2014GL061541.
- Samset, B. H., and G. Myhre (2015), Climate response to externally mixed black carbon as a function of altitude, *J. Geophys. Res. Atmos.*, 120, 2913–2927, doi:10.1002/2014JD022849.
- Schwarz, J. P., B. H. Samset, A. E. Perrring, J. R. Spackman, R. S. Gao, P. Stier, M. Schulz, F. L. Moore, E. A. Ray, and D. W. Fahey (2013), Global-scale seasonally resolved black carbon vertical profiles over the Pacific, *Geophys. Res. Lett.*, 40, 5542–5547, doi:10.1002/2013GL057775.
- Solomon, S., J. S. Daniel, R. R. Neely, J.-P. Vernier, E. G. Dutton, and L. W. Thomason (2011), The persistently variable “background” stratospheric aerosol layer and global climate change, *Science*, 333(6044), 866–870, doi:10.1126/science.1206027.
- Toon, O. B., et al. (1988), A multidimensional model for aerosols—Description of computational analogs, *J. Atmos. Sci.*, 45(15), doi:10.1175/1520-0469(1988).
- Toon, O. B., et al. (2016), Planning, implementation, and scientific goals of the Studies of Emissions and Atmospheric Composition, Clouds and Climate Coupling by Regional Surveys (SEAC<sup>4</sup>RS) field mission, *J. Geophys. Res. Atmos.*, 121, 4967–5009, doi:10.1002/2015JD024297.
- Vernier, J.-P., et al. (2011), Major influence of tropical volcanic eruptions on the stratospheric aerosol layer during the last decade, *Geophys. Res. Lett.*, 38, L12807, doi:10.1029/2011GL047563.
- Vernier, J.-P., et al. (2015), Increase in upper tropospheric and lower stratospheric aerosol levels and its potential connection with Asian pollution, *J. Geophys. Res. Atmos.*, 120, 1608–1619, doi:10.1002/2014JD022372.
- Wilson, J. C., et al. (2008), Steady-state aerosol distributions in the extra-tropical, lower stratosphere and the processes that maintain them, *Atmos. Chem. Phys.*, 8, 6617–6626, doi:10.5194/acp-8-6617-2008.
- Yu, P., O. B. Toon, C. G. Bardeen, M. J. Mills, T. Fan, J. M. English, and R. R. Neely (2015a), Evaluations of tropospheric aerosol properties simulated by the Community Earth System Model with a sectional aerosol microphysics scheme, *J. Adv. Model. Earth Syst.*, 7, 865–914, doi:10.1002/2014MS000421.
- Yu, P., O. B. Toon, R. R. Neely, B. G. Martinsson, and C. A. M. Brenninkmeijer (2015b), Composition and physical properties of the Asian tropopause aerosol layer and the North American tropospheric aerosol layer, *Geophys. Res. Lett.*, 42, doi:10.1002/2015GL063181.
- Ziembka, L. D., et al. (2013), Airborne observations of aerosol extinction by in situ and remote-sensing techniques: Evaluation of particle hygroscopicity, *Geophys. Res. Lett.*, 40, 417–422, doi:10.1029/2012GL054428.
- Zhang, Q., et al. (2007), Ubiquity and dominance of oxygenated species in organic aerosols in anthropogenically-influenced Northern Hemisphere midlatitudes, *Geophys. Res. Lett.*, 34, L13801, doi:10.1029/2007GL029979.